In vitro evaluation of gelatin and chitosan electrospun fibers as artificial guide in peripheral nerve repair: a comparative study

Gnavi, S; Fornasari, B E; Tonda-Turo, C; Laurano, R; Zanetti, M; Ciardelli, G; Geuna, S. In vitro evaluation of gelatin and chitosan electrospun fibers as artificial guide in peripheral nerve repair: a comparative study. JOURNAL OF TISSUE ENGINEERING AND REGENERATIVE MEDICINE. None pp: 0-40.
DOI: 10.1002/term.2351

In vitro evaluation of gelatin and chitosan electrospun fibers to be used as artificial guide in peripheral nerve repair: a comparative study.

Gnavi S. [a,b], Fornasari B.E.[a,b], Tonda-Turo C.[c], Zanetti M.[d], Ciardelli G.[c,e] and Geuna S.[a,b]*

a Department of Clinical and Biological Sciences, University of Torino, Orbassano, 10043, Italy; stefano.geuna@unito.it

b Neuroscience Institute of the Cavalieri-Ottolenghi Foundation, University of Torino, Orbassano, 10043, Italy; sara.gnavi@unito.it; benedettaelena.fornasari@unito.it; stefano.geuna@unito.it

c Politecnico di Torino, Department of Mechanical and Aerospace Engineering, Politecnico of Torino, Torino, 10100 Italy; chiara.tondaturo@polito.it

d Nanostructured Interfaces and Surfaces, Department of Chemistry, University of Torino, Torino, 10100 Italy; marco.zanetti@unito.it

e CNR-IPCF UOS, Pisa, 56124, Italy; gianluca.ciardelli@polito.it

*Corresponding author:

Stefano Geuna, MD

Ospedale San Luigi, Department of Clinical and Biological Sciences

Regione Gonzole 10, 10043 - Orbassano (TO) – ITALY

tel (+39) 011.670.5433/36

fax (+39) 011.903.8639

e-mail: stefano.geuna@unito.it

Keywords: chitosan, gelatin, electrospun fibers, peripheral nerve repair, biomimetic materials, aligned fibres

Abstract

Gelatin and chitosan electrospun nano-fibers can be prepared trough electrospinning technique. Random and aligned fibers mimicking extracellular matrix have been prepared by tuning the collector rotation speed. The effect of fiber alignment on cell

adhesion and proliferation was assessed in vitro by using different Schwann cell (SC) and neuronal models. Moreover, actin cytoskeleton organization, lamellipodia and filipodia formation and axon outgrowth were evaluated. Gelatin and chitosan fibers induced similar adhesion and proliferation rate. Gelatin and chitosan random fibers promoted higher adhesion and proliferation rate induction in comparisons to the aligned ones. Although, gelatin and chitosan fibers alignment resulted in SC and axon oriented growth. Filipodia formation was higher on aligned fibers, suggesting that these substrate can promote higher cell migration in comparison to the random ones. 50B11 neuronal differentiation was better on gelatin fibers, whereas no differences were observed by using DRG explants model. These data suggest both gelatin and chitosan fibers can be promising substrates to be used in peripheral nerve reconstruction.

1. INTRODUCTION

In recent years, the research for effective biomimetic materials for peripheral nerve reconstruction has generated interest in the use of engineered electrospun fibers as alternatives to autografts [1-5]. Electrospun random or align fibers can be easily prepared by electrospinnig technique [6]. In the electrospinning technique, a polymer solution is forced into a capillary tube and subjected to an electric field. When the applied electric field reaches a critical value, the repulsive electrical forces overcome the surface tension forces and, a charged jet of the solution is ejected from the capillary tip [7-9]. Then, an unstable jet occurs in the gap between the Taylor cone and the collector which leads to solvent formation and polymer fiber formation [7-9]. Particularly, random fibers are harvested by using a fixed collector whereas the orientation of nanofibers along a preferred direction can be obtained by using rapidly rotating cylindrical collectors [7-9]. Moreover, fibers diameter can range from nanometer to micrometer size depending on different parameters such as polymer

concentration and solution flow rate [7-9]. Fibers alignment is of interest for tissue engineering purposes in order to give to the cells a preferred growth direction.

In the past years, many synthetic biodegradable polymers, polyglycolic acid (PGA) and polylactic acid (PLA) or polyhydroxybutyrate, and synthetic nonabsorbable materials, such as silicone have been used as artificial nerve guide [3, 5, 10-13]. Food and Drug Administration (FDA) and European Commission (EC) approved a number of biodegradable materials, among them Neurotube™, Neura-Gen™ and Neurolac tubes made of poly(glycolide) (PGA), collagen and poly(dl-lactide-ε-caprolactone), respectively [14-18]. These materials resulted in poor nerve repair and functional recovery in comparison to autograft [19].

During the last years, gelatin and chitosan scaffolds have been used as alternative to synthetic polymers because of their biomimetic properties [20-22].

Biomimetic materials to be used in nerve reconstruction should reduce immunogenicity and inflammatory reactions, be biodegradable, support surgical manipulation, prevent collapse, display a certain degree of porosity to promote efficient exchange of nutrients and waste, and provide topological signalling to cells in order to facilitate reorganization of the inner configuration of the nerve [23-25].

Gelatin is a natural polymer obtained from the thermal denaturation of collagen. However, in comparison to collagen, gelatin is biocompatible, biodegradable, does not provoke immune-rejection reactions, and maintains molecular cues that regulate cell behaviour [21, 24]. However, gelatin can be dissolved in water and the rapid degradation rate of gelatin can be the limiting factor of using gelatin in wound healing. Nevertheless, the degradation can be reduced by using crosslinking agents such as γ-glycidoxypropyltrimethoxysilane (GPTMS) or genipin, thus avoiding the use of acidic solutions and potentially cytotoxic solvents [21, 26-29].

Chitosan is derived from chitin by performing alkaline hydrolysis of acetamide groups. In order to obtain chitosan a combination of high temperature (100°C) with strong aqueous alkali treatments are used to deacetylate chitin [22, 30, 31]. The major limitations in the employ of chitosan in biomedical applications are its low solubility at neutral pH and high viscosity [22, 30]. Despite these disadvantages chitosan has positive properties such as biocompatibility, biodegradability, and no toxicity that make this polymer suitable in biomedical field [22, 30]. Several chitosan products have been approved by the Food and Drug Administration [32]. Moreover, chitosan has been used to produce laser activated film surgical adhesive (SurgiLux) that can be used as an alternative to microsurgery for peripheral nerve repair [33].

Despite biocompatibility and biochemical composition other parameters must be taken in account in innovative inner filler development. Particularly, the topography (three-dimensional architecture) of the inner filler influences cell organization of the regenerating tissue [34-36]. The properties of an internal filler such as fibre composition, diameter and orientation can be diversified to modulate Schwann cell (SC) and axon growth [34-36]. A number of studies have reported that topography plays an important role in controlling adhesion, proliferation, survival and migration of different cell types by affecting formation and distribution of focal adhesion plaques, actin cytoskeleton reorganization and/or lamellipodium and filopodia formation [22, 27, 28, 34-36].

In this study we developed nanofibrous matrices, made up of gelatin or chitosan, characterized by different fibers orientation (random or aligned). RT4-D6P2T schwannoma cell line, primary SC and dorsal root ganglia (DRG) neuronal 50B11 cell line cultures and DRG explants have been set up to perform the experiments. Gelatin and chitosan fibers of 300 nm size were prepared and in vitro and ex vivo were performed to investigate whether the topography and polymer composition modulate SC adhesion, survival and proliferation and neurite outgrowth.

2. MATERIAL AND METHODS

2.1 Gelatin and chitosan fibers preparation

Medical grade CS (molecular weight 200 – 400 kDa, deacetylation degree ≥ 92.6 %) was purchased by Kraeber GmbH & Co. PEO (Mw 900.000 Da), gelatin (type A from porcine skin), (3-Glycidoxypropyl)methyldiethoxysilane (GPTMS) and polyethylene oxide (PEO), dibasic sodium phosphate (DSP), dimethyl sulfoxide (DMSO) and solvents were supplied from Sigma Aldrich.

Crosslinked gelatin nanofibers (GL) were prepared as previously described by author [27, 28, 37].

CS 5 % (w/v) and 3% (w/v) PEO solutions were prepared separately by dissolving CS or PEO in 0.5 M acetic acid solution at room temperature by continuous stirring. After complete solubilisation of each components, a 50/50 (v/v) CS/PEO solution was prepared by mixing equal volumes of CS and PEO solutions to obtain the mixtures with weight ratios of CS to PEO of 62/38; the resultant mixtures were kept under stirring for about 2 hours. A 5% (v/v) of dimethyl sulfoxide was added to the CS/PEO solution as a co-solvent to relax CS chain entanglements and increase the fibre yields and consequently improving the spinnability of the CS-based solution (Bhattarai, et al. 2005b). To increase water stability of nanofibers, a 1 M solution of DSP was added (CS/PEO_DSP) with a concentration of 7.5 % v/v with respect to the natural polymer solution volume as previously described by the authors (Ruini, et al. 2015). Uncrosslinked solution were prepared as control. The final solution was coded as CS. CS nanofibers were prepared through electrospinning system using a voltage of 30kV, a temperature of 37 °C, a nozzle-collector distance of 12 cm and a flow rate of 30

µL/min. Randomly oriented nanofibres were collected on a plane aluminum foil while for aligned nanofibers a rotating mandrel with a speed of 2400 rpm was used.

Both GLO and CS nanofibers were collected on glass coverslips and then sterilized by overnight (O/N) exposure to UV irradiation (UV lamp Technoscientific Co., wavelength 254 nm) and then incubated O/N with complete DMEM.

Before proceeding with cell seeding, fibers samples were sterilized by overnight (O/N) exposure to UV irradiation (UV lamp Technoscientific Co., wavelength 254 nm) and incubated O/N with complete DMEM.

2.2 Scanning electron microscopy and fibers morphology evaluation

Fibers morphology was investigated using Scansion Electronic Microscopy (SEM, LEO 1450VP). Prior to analysis samples were sputtered using gold under vacuum for 100 seconds by Agar Auto Sputter Coater. Micrographs were then analyzed through Image1.44g software to measure fibers diameters.

2.3 Cell cultures

RT4-D6P2T SC line and primary SC were grown on monolayers at 37 °C in a humidified atmosphere of 5% CO_2 as previously described [27, 28]. RT4-D6P2T cell line was purchased from ATCC (American Type Culture Collection, 10801 University Blvd, Manassas, VA 20110-2209) and grown in complete high glucose Dulbecco's modified Eagle's medium (DMEM, Invitrogen) according to the ATCC protocol. SC for primary culture were isolated from sciatic nerves harvested from adult female Wistar rats (Charles River Laboratories, Milan, Italy) weighing approximately 190-220 g. All

procedures were performed in accordance with the Ethics Committee and the European Communities Council Directive of 24 November 1986 (86/609/EEC). Conformed measures were taken to minimize pain and discomfort taking human endpoints for animal suffering and distress into account. The sciatic nerves were harvested, purified and cultured as previously described [27, 37]. The resulted Schwann cells were resuspended in low glucose complete medium and seeded on PLL-coated plates.

2.4 Adhesion assay

RT4-D6P2T and primary SC were seeded in complete DMEM at 4000 and 8000 cells/cm^2 respectively. Adhesion assay was performed on both PLL- (control condition), random or aligned gelatin-fiber coated coverslips and random or aligned chitosan-fiber coated coverslips. After 3h the culture medium was removed and the substrates with attached cells were rinsed with PBS before being fixed by incubation with 4% paraformaldehyde (PFA, Sigma-Aldrich) as described before [27, 28, 37]. After 20 min, the PFA solution was removed and the samples rinsed with PBS. The cells were permeabilized for 10 min with 0.1% Triton X-100 diluted in PBS and blocking solution (normal goat serum, NGS, diluted 1:100 in PBS DAKO X0907) was added for 1 h at room temperature. The cells were stained by O/N incubation with anti-vinculin rabbit polyclonal antibody (diluted 1:600 in PBS, Sigma), followed by 1 h incubation with FITC-conjugated phalloidin (diluted 1:1000 in blocking solution, Millipore, Billerica, MA, USA) at room temperature (diluted 1:1000 in PBS, Millipore) and goat-anti rabbit IgG (H + L) AlexaFluor488 (diluted 1:200 in PBS, Invitrogen). Nuclei were stained with 4,6-

diamidino-2-phenylindole (DAPI, Sigma) diluted 1:1000 in PBS. Cells were photographed under an inverted fluorescence microscope Nikon Eclipse 80i equipped with a Nikon ECLIPSE 80i camera using Image-Pro Plus 6.0 (Media Cybernetics, Silver Spring, MD, USA). Cell numbers were calculated using ImageJ software, averaged and expressed as the number of adherent cells/mm^2 ± standard error of the mean (SEM).

2.5 Proliferation assay

RT4-D6P2T and primary SC were seeded in complete DMEM at 1000 and 2000 cells/cm^2 respectively. Proliferation assay was performed on both PLL- (control), random or aligned gelatin-fiber coated coverslips and random or aligned chitosan-fiber coated coverslips. After 1, 3, 5, and 7 days, cells were fixed, stained, photographed and counted as described in paragraph 2.4. The number of cells counted for each assay was averaged and expressed as cells/mm^2 ± standard error of the mean (SEM).

2.6 MTT assay

RT4-D6P2T and primary SC were plated in 0.2 mL of DMEM containing 10% FBS on both PLL- (control) and chitosan or gelatin random or aligned fibers (experimental group) as previously described [27, 28]. In order to quantify the cell number serial dilution was performed by plating 1×10^3, 2×10^3, 4×10^3, 8×10^3, 1.6×10^4, 3.2×10^4, and 6.4×10^4 per well. After a 1, 3, 5 and 7 day incubation, 10 µL MTT substrate (Sigma, 5 mg/mL in phosphate buffered saline) was added, and the cells incubated at 37 °C for 4 h. The MTT solution was removed and cells washed twice with 0.1 mL of PBS. To dissolve formazan 0.1 mL of dimethyl sulfoxide (DMSO; Sigma) was added to

each well. Spectrophotometric absorbance was measured at 570 nm wavelength, using DMSO as the blank.

2.7 Evaluation of actin cytoskeleton organization

Cell adhesion and morphology were measured using immunocytochemistry staining against anti-vinculin and phalloidin. RT4-D6P2T and primary SC were seeded, fixed and stained as described in paragraph 2.4. 3, 6 or 24 h time points conditions have been performed has described before [27]. For each sample 100 cells were examined making a total of 300 cells for each experimental condition. An arbitrary score was given to each cell and data were expressed as the percentage of cells displaying low, medium or high actin cytoskeleton organization or presence of focal adhesion points ± standard deviation. The entire procedure was carried out in a blind manner as previously described [27].

2.8 Estimation of lamellipodia and filopodia formation

Lamellipodia and filopodia formation was evaluated by direct microscopy of cells stained with anti-S-100β rabbit polyclonal antibody. The cells were seeded, fixed and stained as described in paragraph 2.4. 3, 6 or 24 h time points conditions have been performed has described before [27]. For each sample, 100 cells were examined, making a total of 300 cells for each experimental condition. The data were expressed as percentages of cells displaying only lamellipodia or lamellipodia and filopodia ± standard deviation. The entire procedure was carried out in a blind manner as previously described [27].

2.9 50B11 cultures and differentiation

In order to visualize individual neurite growth cells were plated at low densities on both PLL- (control), random or aligned gelatin-fiber coated coverslips and random or aligned chitosan-fiber coated coverslips. Twenty-four hours after plating, cells were differentiated by adding forskolin (Sigma-Aldrich, 75 μM) to the culture medium as previously described [37]. Twenty-four hours after differentiation, cells were fixed, stained and as described in paragraph 2.4, using β-tubulin mouse mAb (diluted 1:100, in PBS, Sigma) and goat-anti-mouse IgG (H + L) Cy3 (diluted 1:200 in PBS, Invitrogen). Nuclei were stained with DAPI (diluted 1:1000 in PBS, Sigma). Cell number and axon lengths were measured using ImageJ software. Cell number and percentages of differentiated or undifferentiated cells were evaluated in both differentiated and undifferentiated conditions. Counted cells for each assay were averaged and expressed as cells/mm^2 ± standard error of the mean (SEM). Axon length was expressed in μm ± standard error of the mean (SEM).

2.10 DRG explants

DRG explants were harvested from adult female Wistar rats (Charles River Laboratories, Milan, Italy) weighing approximately 190–220 g. All procedures were performed in accordance with the Ethics Committee and the European Communities Council Directive of 24 November 1986 (86/609/EEC). Explants were cultured on coverslips coated with the different fibers matrices. Matrigel coated coverslips were used as negative control. In order to avoid the detachments of the explants 100 μl matrigel® were added to the top of the cultures. After 1 hour of incubation at 37 °C to

allow the matrigel® to polymerize, complete F12-BME medium (2 ml) was added. Complete F12–BMEmedium I s composed by F12 and BME media (Gibco) in a 50:50 ratio containing 1% bovine serum albumin (BSA, Sigma), 0.5 g/ml D-glucose (Sigma), 100 U/ml penicillin and streptomycin (Sigma), 1 mg/100 ml putrescine (Sigma), 2 mM L-glutamine (Sigma), 2 ml of 100× insulin–selenium–transferrin (Gibco) and 0.125 ng/ml vitamin C. Culture medium was added, either without growth factors (negative control) or containing 50 ng NGF/ml (positive control).

After 48 h of incubation, the explants were fixed with 4% PFA, for 20 min at RT. Axons were stained immunocytochemically as described in paragraph 2.4, using β-tubulin mouse mAb (diluted 1:100, in PBS, Sigma) and goat-anti-mouse IgG (H + L) AlexaFluor488 (diluted 1:200 in PBS, Invitrogen). Nuclei were stained with 4',6-diamidino-2-phenylindole (diluted 1:1000 in PBS, Sigma). For quantification, the whole explants were acquired through an inverted optical video-confocal microscope (ViCo, Nikon Eclipse 80i) equipped with a Nikon ECLIPSE 80i camera using Image-Pro Plus 6.0 (Media Cybernetics USA). Axon density, sprouting area and axon lengths were measured using ImageJ software as described elsewhere [38, 39]. Axon density was expressed as pixels occupied by axons ± SEM. Sprouting area was expressed as the ratio between DRG axon occupied area and DRG body area ± SEM. Axon length was expressed in µm ± SEM.

2.11 Confocal microscopy

Samples were observed with a Nikon Eclipse E800 epifluorescence microscope under appropriate filters and a Leica TCS SP5 confocal laser scanning microscope (Leica,

Mannheim, Germany) using a 40× Plan-NEOFLUAR objective (numerical aperture (NA) = 1.25) or 63× Plan-NEOFLUAR objective (numerical aperture (NA) = 1.40). High-resolution images were acquired (1024 × 1024 pixels) at 100 Hz.

2.12 Statistics

The experiments were repeated 3 times independently and included 3 sets of samples. Each set included three control PLL-, three random gelatin fiber matrix-, three align gelatin fiber matrix-, three random chitosan fiber matrix-, and three align chitosan fiber matrix-coated coverslips. The data are expressed as mean ± standard error of the mean (SEM). GraphPad Prism® software was used for one or two way analysis of variance (ANOVA). Values of * $p < 0.05$, ** $p < 0.01$, *** $p < 0.001$ were considered statistically significant.

3. RESULTS AND DISCUSSION

3.1 Gelatin and chitosan polymer can be easily used to prepare electrospun nano-fibers

GL and CS nanofibers were obtained with no defects on the fiber surface **(Figure 1).** Despite the differences in materials and parameters used, the average diameter of the different fibers was similar and did not show significant differences **(Table 1).**

3.2 Gelatin and chitosan nano-fibers promote similar Schwann cells adhesion rate

RT4-D6P2T and primary SC were cultured on control condition (polylysine coated coverslips), gelatin and chitosan random and aligned fibers. After 3 h,

the adherent cells were fixed, stained and counted. The alignment of gelatin and chitosan electrospun fibers decreased the number of adherent cells for RT4-D6P2T and primary SC cultures **(Figure 2).** RT4-D6P2T cells seeded on aligned gelatin fibers displayed lower adhesion rate than under control conditions ($p<0.05$), gelatin random fibers ($p<0.01$), and chitosan random fibers ($p<0.05$) **(Figure 2).** RT4-D6P2T cells seeded on aligned chitosan fibers displayed lower adhesion rate than under control conditions ($p<0.01$), gelatin random fibers ($p<0.01$), and chitosan random fibers ($p<0.05$) **(Figure 2).**

Primary SC seeded on aligned gelatin fibers displayed lower adhesion rate than under control conditions ($p<0.001$), gelatin random fibers ($p<0.001$), and chitosan random fibers ($p<0.01$) **(Figure 2).** Primary SC seeded on aligned chitosan fibers displayed lower adhesion rate than under control conditions ($p<0.001$), gelatin random fibers ($p<0.001$), and chitosan random fibers ($p<0.001$) **(Figure 2).** Moreover, primary SC seeded on chitosan aligned fibers displayed lower adhesion rate in comparison to gelatin aligned fibers ($p<0.05$) **(Figure 2).** Altogether these results showed that gelatin and chitosan random fibers promote SC adhesion reaching adhesion rate levels similar to cells cultured on control condition. Aligned fibers still promote SC adhesion even if adhesion rates are lower than those reached by cells cultured on control condition and random fibers. This can be due to the different topography of the aligned fibers in comparison to the random ones [35, 40]. Particularly, fibers alignment provide less contact points to the cells thus resulting in lower adhesion rate [27, 35, 40]. On the other hand random fibers distribution results

in a complex network formation between fibers proving many contact points to the adhering cells [27, 35, 36, 40]. Concerning cell morphology, fiber alignment results in adherent cells align their body parallel to the direction of the fiber whereas cells seeded on random fibers display a spread morphology in accordance with previous study [27, 37, 41].

3.3 Chitosan nano-fibers resulted in lower Schwann cell proliferation rate in comparison with gelatin nano-fibers

RT4-D6P2T and primary SC cultures were cultured on control condition (polylysine coated coverslips), gelatin and chitosan random fibers and aligned fibers. After 1, 3, 5 and 7 days in vitro (DIV) the proliferating cells were fixed, stained and counted **(Figures 3 and 4).** The alignment of gelatin and chitosan electrospun fibers decreased the number of proliferating cells for RT4-D6P2T and primary SC cultures. Moreover, RT4-D6P2T and primary SC displayed lower proliferation rate when cultured on chitosan fibers, both random and aligned in comparison to control condition and random gelatin fibers. Two way Anova analysis reported in **supplementary table 1** show that the different fiber substrate ($p<0.001$) and the time ($p<0.001$) affect RT4-D6P2T cell proliferation. Interaction between the different fiber substrate and time accounts 13.04% of the total variance affecting significantly cell proliferation ($p<0.001$).

Particularly, RT4-D6P2T cells seeded on random gelatin fibers, aligned gelatin fibers, or aligned chitosan fibers displayed lower proliferation rate than under control condition and gelatin random fibers both at 5 and 7 DIV ($p<0.001$), and

chitosan random fibers ($p<0.05$) (Two way Anova analysis is reported in **supplementary table 1**. RT4-D6P2T cells seeded on aligned chitosan fibers displayed lower proliferation rate than under gelatin aligned fibers at 5 ($p<0.05$) and 7 ($p<0.001$) DIV (Two way Anova analysis is reported in **supplementary table 1**. Finally, RT4-D6P2T cells seeded on aligned chitosan fibers displayed lower proliferation rate than under chitosan random fibers at 5 ($p<0.01$) and 7 ($p<0.001$) DIV (Two way Anova analysis is reported in **supplementary table 1**. Similar results have been obtained by using primary SC cultures **(Figure 4),** Two way Anova analysis is reported in the **Supplementary table 2).**

In order to evaluate cell vitality MTT assay has been performed on both RT4-D6P2T and primary SC cultured on the different substrates **(Figures 3 and 4).** MTT results are in accordance with proliferation assay data for both RT4-D6P2T and primary SC (MTT assay two-way ANOVA results for RT4-D6P2T and primary SC are reported in **supplementary table 3 and 4, respectively**. Altogether proliferation and MTT assay results demonstrate that the different substrates allow SC proliferation and vitality in accordance with previous data [27, 37]. Although, random gelatin fibers seems to be the better substrate for SC proliferation and vitally followed by gelatin aligned fibers, chitosan random fibers and chitosan aligned fibers. The higher cell proliferation on random fibers can be due to the fibers topography that, as already discussed, provides more contact point to the proliferating cells [35, 36, 40]. Even if random fibers induces higher proliferation rate a number of study reported that fibers

alignment promote better nerve regeneration [22, 41-45]. Particularly, fluorescent images show that SC cultured on align fibers arrange themselves in parallel bands with elongate cell body parallel to the direction of the fibers. Thus, align fibers can be use to promote band of Bungner formation in vivo enhancing nerve regeneration process [46, 47].

3.4 Gelatin and chitosan nano-fibers alignment resulted in lower actin cytoskeleton organization and fewer focal adhesion points in comparison with gelatin nano-fibers.

Both RT4-D6P2T **(Figure 5)** and primary SC **(Figure 6)** cultured under control conditions and on aligned and random gelatin and chitosan fibers. Cells seeded on control condition and random gelatin fibers displayed higher actin cytoskeleton organization and many focal adhesion points then those cultured on gelatin aligned fibers and chitosan fibers both random and aligned. This trend was maintained at all the time points tested (3, 6 and 24 h). Two way Anova analysis is reported in **supplementary table 11-16** for RT4-D6P2T cells and in **supplementary table 17-22** for primary SC. Finally, actin cytoskeleton staining showed that cells cultured under control conditions and on gelatin radom fibers displayed a spread morphology whereas those cultured aligned and chitosan fibers had an elongated morphology. These data accord with the adhesion assay results and with previous studies [27, 37, 41, 42]. Several authors reported that actin cytoskeleton organization play an important role in lamellipodia and filipodia formation [48-51]. Since a different actin

cytoskeleton organization on SC cultured on the different substrate has been observed immunofluorescence assay to investigate if there were differences on lamellipodia and filipodia formation on the different substrates have been performed.

3.5 Gelatin and chitosan nano-fibers alignment enhances filopodia formation

Lamellipodia and filipodia formation have been evaluated by culturing both primary SC and RT4-D6P2T cell line on the different substrate. Results showed that fiber alignment led to more cells displaying filopodia in both RT4-D6P2T **(Figure 7)** and primary SC **(Figure 8).** This trend was maintained at all the time points tested (3, 6 and 24 h). Two way Anova analysis is reported in **(Supplementary table 23-25 and 26-28)** for RT4-D6P2T and primary SC respectively). Lamellipodia are motile strutures formed by a thin sheet of cytoplasm filled with a criss-cross arranged network of actin filaments[52]. Filopodia consist of rod-shaped cell projections full of linear actin filaments and their formation often is come with lamellipodia [52]. Several studied reported that filipodia formation is associated to cell motility and migration [50, 52-54], thus our data suggest that fiber alignment may induce SC migration.

3.6 Gelatin nano-fibers resulted in higher 50B11 cell differentiation and neurites length in comparison with chitosan nano-fibers

50B11 were seeded under control condition, and also on aligned and random gelatin and chitosan fibers. After 24 hours, 50B11 displayed high adhesion rate

under the different substrate without any statistical difference between groups **(Supplementary table 8).** The alignment of gelatin and chitosan fibers did not affect the number of adherent 50B11 cells **(Figure 9).** Addition of forskolin resulted in 50B11 differentiation under all conditions tested **(Figure 9)** without any statistical difference **(Supplementary table 8).** After forskolin addition, 50B11 cells stopped proliferating and started differentiating, resulting in a reduced cell number compared with non-treated conditions (One way Anova statistics is reported in **Figure 9**). The number of differentiated 50B11 cells is slightly decreased when 50B11 cells are cultured on gelatin align fibers in comparison to control condition ($p<0.05$). 50B11 neurite length was higher on control condition, gelatin random fibers and gelatin aligned fibers in comparison to chitosan random and aligned fibers **(figure 9).** According with these results, confocal images showed that aligned fibers made neurites aligned in parallel to the direction of the fibers **(figure 9**). In order to understand if fibers itself can induce cell differentiation the number of differentiated cells in presence or without forskolin in culture medium was evaluated**.** Results, expressed as percentage of differentiated and undifferentiated cells, show that with foskolin addition there are high percentages of differentiated cells without any statistical difference between the different substrate **(Supplementary table 9).** When 50B11 cells are cultured without forskolin there are higher percentages of undifferentiated cells **(Figure 9).** Although gelatin aligned fibers seems to induce 50B11 differentiation in comparison with control condition, gelatin random fibers and, chitosan

random and aligned fibers ($p<0.001$) **(Supplementary Table 10).** Gelatin random fibers seems to induce 50B11 differentiation in comparison with control condition and, chitosan random and aligned fibers ($p<0.001$) **(Supplementary Table 10).** These results suggest that gelatin random and align fibers topography may induce neuron differentiation and neurite alignment in accordance with several studies [37, 41-44, 55, 56]. Particularly, longitudinally aligned nanofibers promote ordered neuritis outgrowth [44], PC12 and DRGs alignment [42] and parallel axonal growth and hMSC and PC-12 cells neurogenic differentiation [41].

3.7 Gelatin and chitosan nano-fibers resulted in similar DRG neurites growth and alignment

DRG explants were cultured on control condition (polylysine coated coverslips), gelatin and chitosan random fibers and aligned fibers with or without NGF in culture medium. After 48 h, the explants were fixed, stained and neurite length, neurite occupied area and neurite area ratio were quantified. Neurite length, neurite occupied area and neurite area ratio were higher when DRG explants were cultured in presence of NGF (One-way Anova statistics is reported in **figure 10).** When DRG explants were cultured in presence of NGF neurite length was higher on gelatin and chitosan aligned fibers in comparison with all the other tested condition **(Supplementary table 5).** There are no difference between neurite length of DRG explants cultured on gelatin and chitosan aligned fibers in presence of NGF **(Supplementary table 5).** Moreover,

when DRG explants were cultured without NGF neurite length was higher on gelatin aligned fibers, chitosan random and aligned fibers in comparison to control condition and gelatin random fibers **(Supplementary table 5).**

When DRG explants were cultured in presence of NGF neurite occupied area was higher on control condition and random fibers in comparison to aaligned fibers **(Supplementary table 6)**. When DRG explants were cultured without NGF neurite occupied area was lower on control condition and aligned fibers in comparison with the other tested substrate **(Supplementary table 6)**. Similar results have been obtained by evaluating the ratio between the area occupied by the neuritis and the area occupied by the DRG body **(Supplementary table 7).** Fluorescence images show that aligned fibers result in parallel neurites outgrowth in accordance with literature data [41, 42, 56].

CONCLUSION

Reported data show that both gelatin and chitosan fibers can be promising filler to be used in peripheral nerve conduits development. Particularly, aligned fibers induce SC and axon oriented growth with cell body parallel to the direction of the fibers. Gelatin fibers resulted in better 50B11 neuronal differentiation in comparison to chitosan fibers. Although, DRG neurite outgrowth was similar on the different tested substrates. Concerning chitosan fibers we observed an oriented growth that can be due to both the polymer biomimetic and biochemical intrinsic properties [22, 57]. Both chitosan and gelatin have been widely used for peripheral nerve repair displaying high biocompatibility [22-24, 33, 42, 44, 57]. In this work gelatin and chitosan fibers have

been tested showing that depending on their morphology and biochemical composition they can induce and promote different regenerative events (i.e. SC adhesion, SC proliferation, neuronal differentiation and growth). In conclusion, all the tested substrate can be used for nerve regeneration purpose depending on the kind of lesion and consequently on the regenerative events that can be useful to induce.

ACKNOWLEDGMENTS

We thank Ahmet Höke (Department of Neurology, School of Medicine, Johns Hopkins University, Baltimore, USA) for providing the 50B11 cell line. We acknowledge a research grant for Sara Gnavi from the Franco and Marilisa Caligara Foundation. This work also received funding from the European Community's Seventh Framework Programme (FP7-HEALTH-2011) under grant agreement n 278612 (BIOHYBRID).

REFERENCES

1. **Gu, X., et al., *Construction of tissue engineered nerve grafts and their application in peripheral nerve regeneration.* Prog Neurobiol, 2011. 93(2): p. 204-30.**
2. **Ichihara, S., Y. Inada, and T. Nakamura, *Artificial nerve tubes and their application for repair of peripheral nerve injury: an update of current concepts.* Injury, 2008. 39 Suppl 4: p. 29-39.**
3. **Jiang, X., et al., *Current applications and future perspectives of artificial nerve conduits.* Exp Neurol, 2010. 223(1): p. 86-101.**
4. **Siemionow, M. and G. Brzezicki, *Chapter 8: Current techniques and concepts in peripheral nerve repair.* Int Rev Neurobiol, 2009. 87: p. 141-72.**
5. **Biazar, E., et al., *Types of neural guides and using nanotechnology for peripheral nerve reconstruction.* Int J Nanomedicine, 2010. 5: p. 839-52.**
6. **Bhardwaj, N. and S.C. Kundu, *Electrospinning: a fascinating fiber fabrication technique.* Biotechnol Adv, 2010. 28(3): p. 325-47.**
7. **Adomaviciute, E. and R. Milasius, *The influence of applied voltage on poly(vinyl alcohol) (PVA) nanofibre diameter.* Fibres & Textiles in Eastern Europe, 2007. 15(5-6): p. 69-72.**
8. **Yarin, A.L., S. Koombhongse, and D.H. Reneker, *Bending instability in electrospinning of nanofibers.* Journal of Applied Physics, 2001. 89(5): p. 3018-3026.**

9. Christopherson, G.T., H. Song, and H.Q. Mao, *The influence of fiber diameter of electrospun substrates on neural stem cell differentiation and proliferation.* Biomaterials, 2009. 30(4): p. 556-64.
10. Cunha, C., S. Panseri, and S. Antonini, *Emerging nanotechnology approaches in tissue engineering for peripheral nerve regeneration.* Nanomedicine, 2011. 7(1): p. 50-9.
11. Dahlin, L.B., L. Anagnostaki, and G. Lundborg, *Tissue response to silicone tubes used to repair human median and ulnar nerves.* Scand J Plast Reconstr Surg Hand Surg, 2001. 35(1): p. 29-34.
12. Lundborg, G., et al., *Tubular repair of the median or ulnar nerve in the human forearm: a 5-year follow-up.* J Hand Surg Br, 2004. 29(2): p. 100-7.
13. Pfister, L.A., et al., *Nerve conduits and growth factor delivery in peripheral nerve repair.* J Peripher Nerv Syst, 2007. 12(2): p. 65-82.
14. Archibald, S.J., et al., *A Collagen-Based Nerve Guide Conduit for Peripheral-Nerve Repair - an Electrophysiological Study of Nerve Regeneration in Rodents and Nonhuman-Primates.* Journal of Comparative Neurology, 1991. 306(4): p. 685-696.
15. Archibald, S.J., et al., *Monkey Median Nerve Repaired by Nerve Graft or Collagen Nerve Guide Tube.* Journal of Neuroscience, 1995. 15(5): p. 4109-4123.
16. Bertleff, M.J.O.E., M.F. Meek, and J.P.A. Nicolai, *A prospective clinical evaluation of biodegradable neurolac nerve guides for sensory nerve repair in the hand.* Journal of Hand Surgery-American Volume, 2005. 30A(3): p. 513-518.
17. Hernandez-Cortes, P., et al., *Failed Digital Nerve Reconstruction by Foreign Body Reaction to Neurolac (R) Nerve Conduit.* Microsurgery, 2010. 30(5): p. 414-416.
18. Weber, R.A., et al., *A randomized prospective study of polyglycolic acid conduits for digital nerve reconstruction in humans.* Plastic and Reconstructive Surgery, 2000. 106(5): p. 1036-1045.
19. Daly, W., et al., *A biomaterials approach to peripheral nerve regeneration: bridging the peripheral nerve gap and enhancing functional recovery.* J R Soc Interface, 2012. 9(67): p. 202-21.
20. Chevallay, B. and D. Herbage, *Collagen-based biomaterials as 3D scaffold for cell cultures: applications for tissue engineering and gene therapy.* Med Biol Eng Comput, 2000. 38(2): p. 211-8.
21. Chiono, V., et al., *Genipin-crosslinked chitosan/gelatin blends for biomedical applications.* J Mater Sci Mater Med, 2008. 19(2): p. 889-98.
22. Gnavi, S., et al., *The use of chitosan-based scaffolds to enhance regeneration in the nervous system.* Int Rev Neurobiol, 2013. 109: p. 1-62.
23. Chiono, V., C. Tonda-Turo, and G. Ciardelli, *Chapter 9: Artificial scaffolds for peripheral nerve reconstruction.* Int Rev Neurobiol, 2009. 87: p. 173-98.
24. Ciardelli, G. and V. Chiono, *Materials for peripheral nerve regeneration.* Macromol Biosci, 2006. 6(1): p. 13-26.
25. Zhang, B.G., et al., *Recent advances in nerve tissue engineering.* Int J Artif Organs, 2014. 37(4): p. 277-91.
26. Gnavi, S., et al., *Gelatin-based hydrogel for vascular endothelial growth factor release in peripheral nerve tissue engineering.* J Tissue Eng Regen Med, 2014.
27. Gnavi, S., et al., *The influence of electrospun fibre size on Schwann cell behaviour and axonal outgrowth.* Mater Sci Eng C Mater Biol Appl, 2015. 48: p. 620-31.
28. Tonda-Turo, C., et al., *Crosslinked gelatin nanofibres: preparation, characterisation and in vitro studies using glial-like cells.* Mater Sci Eng C Mater Biol Appl, 2013. 33(5): p. 2723-35.

29. **Zhang, S., et al., *Gelatin nanofibrous membrane fabricated by electrospinning of aqueous gelatin solution for guided tissue regeneration.* J Biomed Mater Res A, 2009. 90(3): p. 671-9.**
30. **Khor, E. and L.Y. Lim, *Implantable applications of chitin and chitosan.* Biomaterials, 2003. 24(13): p. 2339-2349.**
31. **Nishi, N., et al., *Highly Phosphorylated Derivatives of Chitin, Partially Deacetylated Chitin and Chitosan as New Functional Polymers - Preparation and Characterization.* International Journal of Biological Macromolecules, 1986. 8(5): p. 311-317.**
32. **Dornish, M.K., D. S. Arepalli, S. R., *Regulatory Status of Chitosan and Derivatives, in Chitosan-Based Systems for Biopharmaceuticals: Delivery, Targeting and Polymer Therapeutics* (eds B. Sarmento and J. das Neves), John Wiley & Sons, Ltd, Chichester, UK. , 2012.**
33. **Foster, L.J.R. and E. Karsten, *A Chitosan Based, Laser Activated Thin Film Surgical Adhesive, 'SurgiLux': Preparation and Demonstration.* Jove-Journal of Visualized Experiments, 2012(68).**
34. **Agarwal, S.W., H. Greiner, A., *Use of electrospinning technique for biomedical applications.* Polymer, 2008. 49: p. 5603-5621.**
35. **Bacakova, L., et al., *Modulation of cell adhesion, proliferation and differentiation on materials designed for body implants.* Biotechnol Adv, 2011. 29(6): p. 739-67.**
36. **Harvey, A.G., E.W. Hill, and A. Bayat, *Designing implant surface topography for improved biocompatibility.* Expert Rev Med Devices, 2013. 10(2): p. 257-67.**
37. **Gnavi, S., et al., *The Effect of Electrospun Gelatin Fibers Alignment on Schwann Cell and Axon Behavior and Organization in the Perspective of Artificial Nerve Design.* Int J Mol Sci, 2015. 16(6): p. 12925-42.**
38. **Gilardino, A., et al., *Specificity of the second messenger pathways involved in basic fibroblast growth factor-induced survival and neurite growth in chick ciliary ganglion neurons.* J Neurosci Res, 2009. 87(13): p. 2951-62.**
39. **Zamburlin, P., et al., *Temporal dynamics of neurite outgrowth promoted by basic fibroblast growth factor in chick ciliary ganglia.* J Neurosci Res, 2006. 84(3): p. 505-14.**
40. **Rahmany, M.B. and M. Van Dyke, *Biomimetic approaches to modulate cellular adhesion in biomaterials: A review.* Acta Biomater, 2013. 9(3): p. 5431-7.**
41. **Cirillo, V., et al., *Optimization of fully aligned bioactive electrospun fibers for "in vitro" nerve guidance.* J Mater Sci Mater Med, 2014. 25(10): p. 2323-32.**
42. **Dinis, T.M., et al., *Complementary effects of two growth factors in multifunctionalized silk nanofibers for nerve reconstruction.* PLoS One, 2014. 9(10): p. e109770.**
43. **Genchi, G.G., et al., *PC12 neuron-like cell response to electrospun poly(3-hydroxybutyrate) substrates.* J Tissue Eng Regen Med, 2015. 9(2): p. 151-61.**
44. **Huang, C., et al., *Nerve guidance conduits from aligned nanofibers: improvement of nerve regeneration through longitudinal nanogrooves on a fiber surface.* ACS Appl Mater Interfaces, 2015. 7(13): p. 7189-96.**
45. **Neal, R.A., et al., *Alignment and composition of laminin-polycaprolactone nanofiber blends enhance peripheral nerve regeneration.* J Biomed Mater Res A, 2012. 100(2): p. 406-23.**
46. **de Ruiter, G.C., et al., *Designing ideal conduits for peripheral nerve repair.* Neurosurg Focus, 2009. 26(2): p. E5.**
47. **Deumens, R., et al., *Repairing injured peripheral nerves: Bridging the gap.* Prog Neurobiol, 2010. 92(3): p. 245-76.**

48. **Defilippi, P., et al., *Actin cytoskeleton organization in response to integrin-mediated adhesion.* Microsc Res Tech, 1999. 47(1): p. 67-78.**
49. **Fabry, B., et al., *Focal Adhesion Kinase Stabilizes the Cytoskeleton.* Biophysical Journal, 2011. 101(9): p. 2131-2138.**
50. **Mullins, R.D. and S.D. Hansen, *In vitro studies of actin filament and network dynamics.* Curr Opin Cell Biol, 2013. 25(1): p. 6-13.**
51. **Parsons, J.T., A.R. Horwitz, and M.A. Schwartz, *Cell adhesion: integrating cytoskeletal dynamics and cellular tension.* Nat Rev Mol Cell Biol, 2010. 11(9): p. 633-43.**
52. **Mattila, P.K. and P. Lappalainen, *Filopodia: molecular architecture and cellular functions.* Nat Rev Mol Cell Biol, 2008. 9(6): p. 446-54.**
53. **Mitra, S.K., D.A. Hanson, and D.D. Schlaepfer, *Focal adhesion kinase: In command and control of cell motility.* Nature Reviews Molecular Cell Biology, 2005. 6(1): p. 56-68.**
54. **Qu, J.W., D. Wang, H. Dong, Y. Zhang, F. Zuo, B. Zhang, H. , *Electrospun silk fibroin nanofibers in different diameters support neurite outgrowth and promote astrocyte migration.* J Biomed Mater Res Part A 2013. 101A: p. 2667–2678.**
55. **Mahairaki, V., et al., *Nanofiber matrices promote the neuronal differentiation of human embryonic stem cell-derived neural precursors in vitro.* Tissue Eng Part A, 2011. 17(5-6): p. 855-63.**
56. **Xie, J., et al., *Neurite outgrowth on nanofiber scaffolds with different orders, structures, and surface properties.* ACS Nano, 2009. 3(5): p. 1151-9.**
57. **Meyer, C., et al., *Chitosan-film enhanced chitosan nerve guides for long-distance regeneration of peripheral nerves.* Biomaterials, 2016. 76: p. 33-51.**

	GL random fibers	GL aligned fibers	CS random fibers	CS aligned fibers
Fiber size (nm)	242± 35nm	204 ± 48 nm	167 ± 34 nm	159± 41 nm

Table 1. Average size of GL and CS nano-fibers.

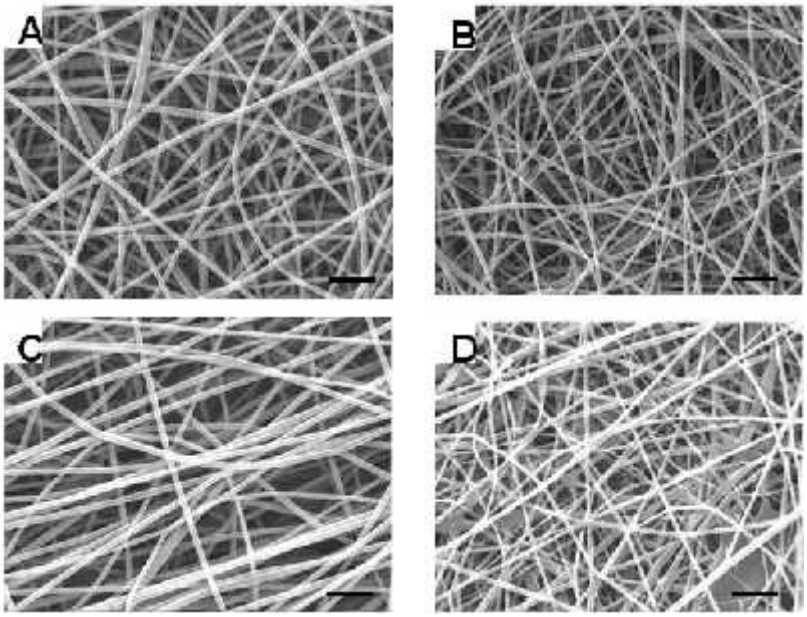

Figure 1 SEM micrographs randomly oriented (A) GL and CS (B) nano-fibers and aligned (C) GL and (D) CS nano-fibers. Scale bars: 2µm.

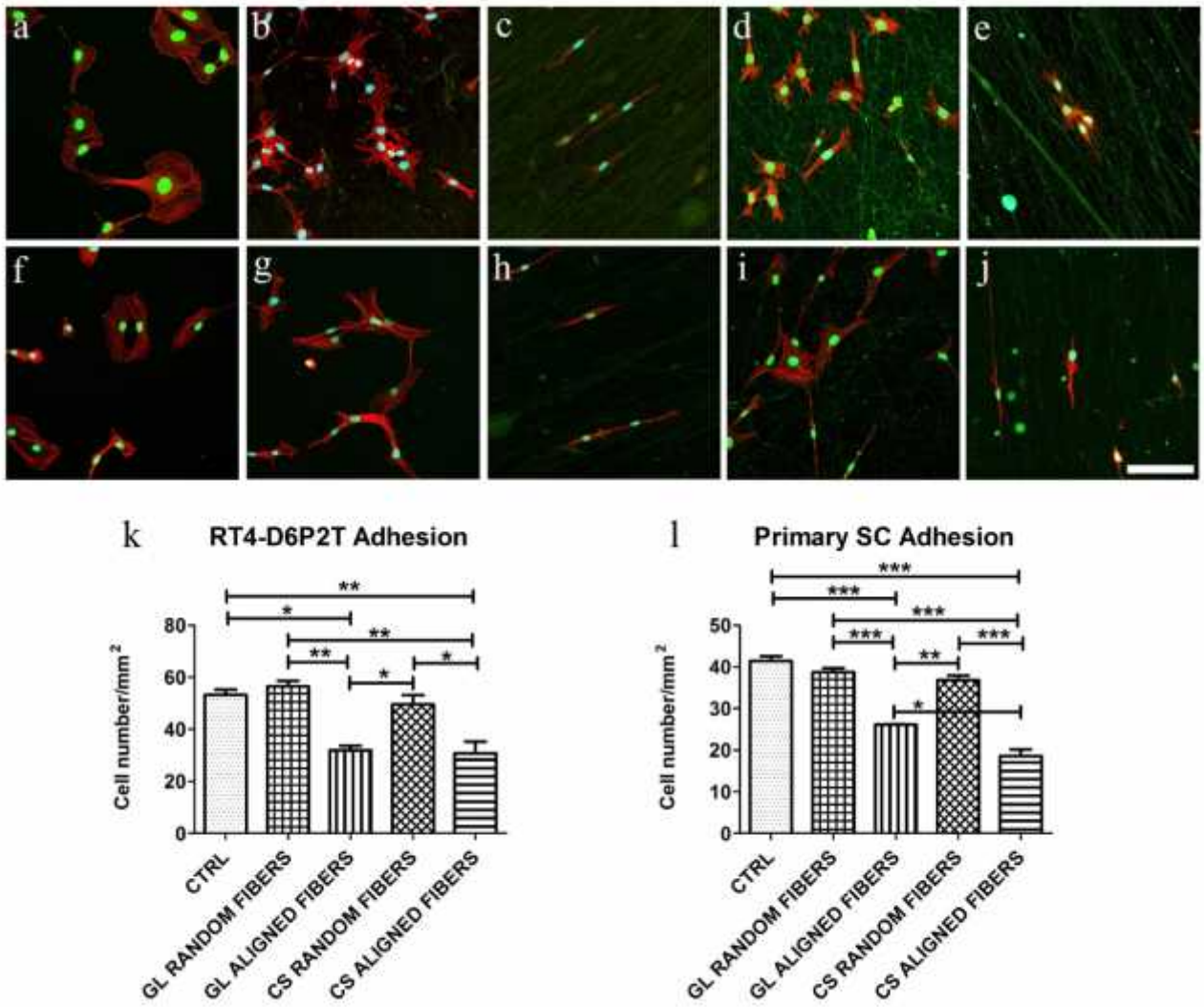

Figure 2. Adhesion assay. Fluorescence images after vinculin (green), phalloidin (red) and DAPI (blue) staining of RT4-D6P2T (a-e) and primary SC culture (f-j) on poly-l-lysine coated coverslips (control condition, a and f), gelatin random fibers (b and g), gelatin aligned fibers (c and h), chitosan random fibers (d and i), and chitosan aligned fibers (e and j). Fibers substrates appear green due to material autofluorescence. Images were acquired at 40X magnification. Scale bar: 100 µm. Numbers of adhering RT4-D6P2T (k) and primary SC cells (l) are reported. Cell number is expressed as cells/mm^2 ± standard error of the mean (SEM). One-way ANOVA was used for statistical analysis. Asterisks denote statistically significant differences with *$p \leq 0.05$, **$p \leq 0.01$ and ***$p \leq 0.001$.

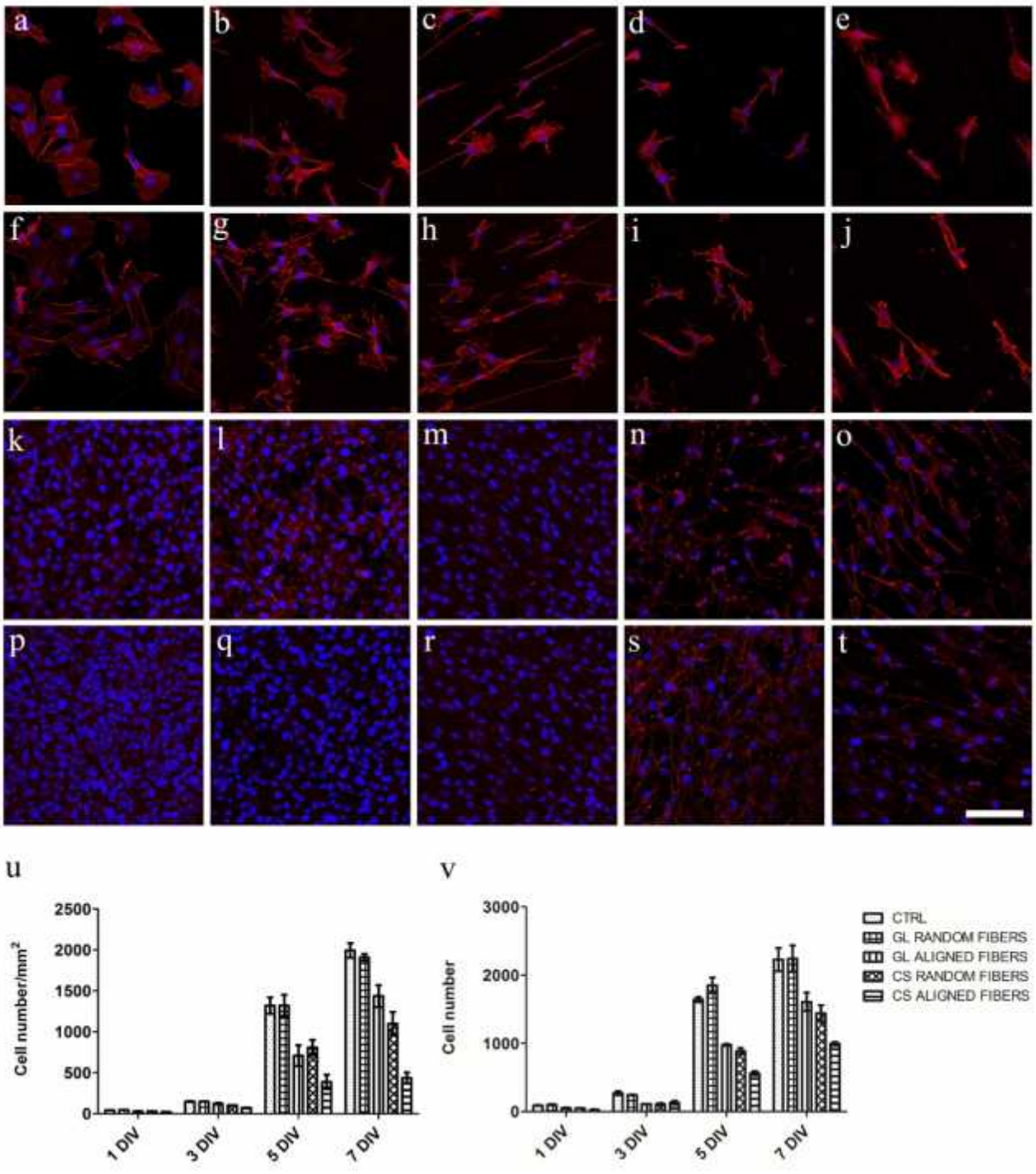

Figure 3. RT4-D6P2T proliferation and MTT assay. Fluorescence images after phalloidin (red) and DAPI (blue) staining of RT4-D6P2T (a-t), on poly-l-lysine coated coverslips (control condition, a, f, k, and p), gelatin random fibers (b, g, l, and q), gelatin aligned fibers (c, h, m, and r), chitosan random fibers (d, i, n, and s), and chitosan aligned fibers (e, j, o, and t) after 1 (a-e), 3 (e-j), 5 (k-o) and 7 (p-q) DIV (days in vitro). Images were acquired at 40X magnification. Scale bar: 100 µm. Numbers of proliferating RT4-D6P2T are reported as cells/mm^2 ± standard error of the mean (SEM) (u). Cell vitality was quantified trough MTT assay

and reported as cell number± standard error of the mean (SEM) (v). Two-way ANOVA was used for statistical analysis *p ≤ 0.05, **p ≤ 0.01 and ***p ≤ 0.001 (Supplementary table 1 and 3).

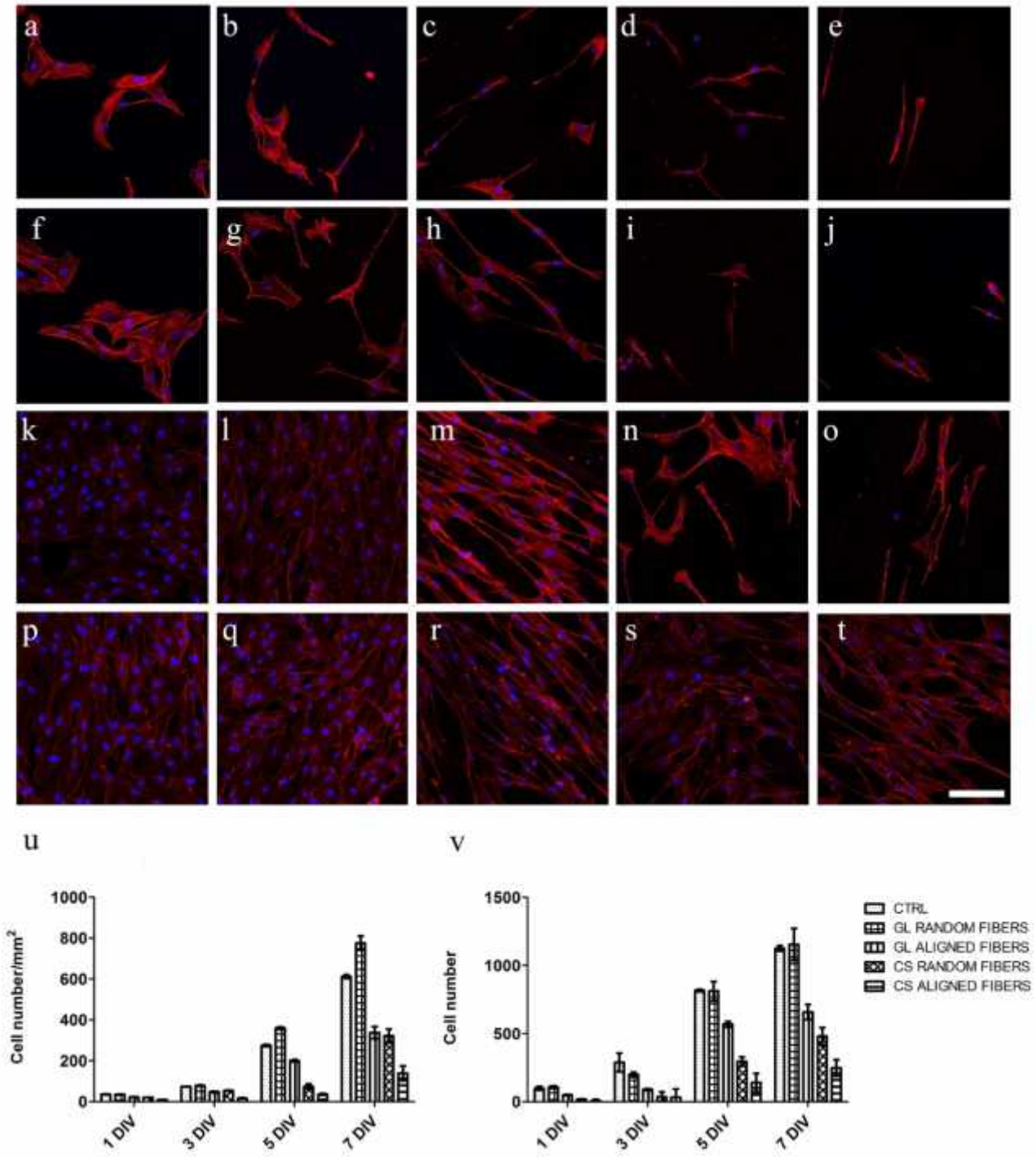

Figure 4. Primary SC proliferation and MTT assay. Fluorescence images after phalloidin (red) and DAPI (blue) staining of SC (a-t), on poly-l-lysine coated coverslips (control condition, a, f, k, and p), gelatin random fibers (b, g, l, and q), gelatin aligned fibers (c, h, m, and r), chitosan random fibers (d, i, n, and s),

and chitosan aligned fibers (e, j, o, and t) after 1 (a-e), 3 (e-j), 5 (k-o) and 7 (p-q) DIV (days in vitro). Images were acquired at 40X magnification. Scale bar: 100 µm. Numbers of proliferating SC are reported as cells/mm^2 ± standard error of the mean (SEM) (u). Cell vitality was quantified trough MTT assay and reported as cell number± standard error of the mean (SEM) (v). Two-way ANOVA was used for statistical analysis *p ≤ 0.05, **p ≤ 0.01 and ***p ≤ 0.001 (Supplementary tables 2 and 4).

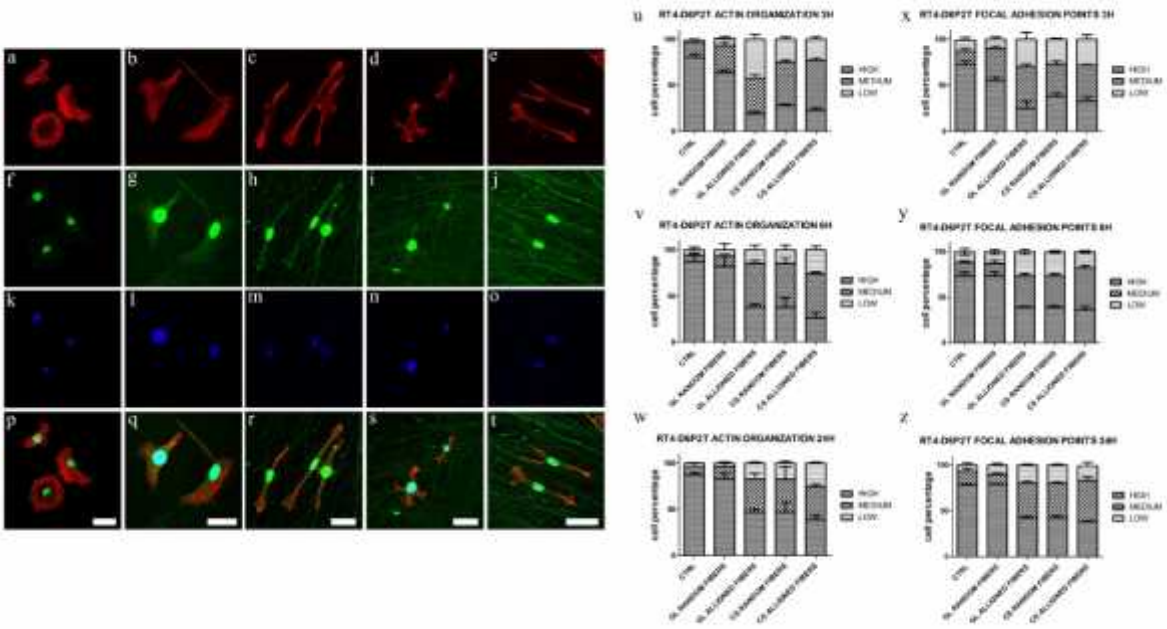

Figure 5. RT4-D6P2T actin cytoskeleton and focal adhesion points organization. Fluorescence images following phalloidin-actin (red), vinculin (green) and DAPI (blue) staining of RT4-D6P2T on poly-l-lysine coated coverslips (control condition, a, f, k and p), gelatin random fibers (b, g, l and q), gelatin aligned fibers (c, h, m and r), chitosan random fibers (d, i, n and s), and chitosan aligned fibers (e, j, o and t). Fibers substrates appear green due to material autofluorescence. Images were acquired at 60X magnification with different zoom. Scale bar: 40 µm. Percentages of cells with low, medium or high actin cytoskeleton organization ± standard error of the mean (SEM) 3 (u), 6 (v) and 24 (w) h after seeding are reported. Percentages of cells with low, medium or high numbers of focal adhesion points ± standard error of the mean (SEM) 3 (x), 6 (y) and 24 (z) h after seeding are also reported. One-way ANOVA was used for statistical

analysis. Asterisks denote statistically significant differences with *p ≤ 0.05, **p ≤ 0.01 and ***p ≤ 0.001 (Supplementary tables 11-16).

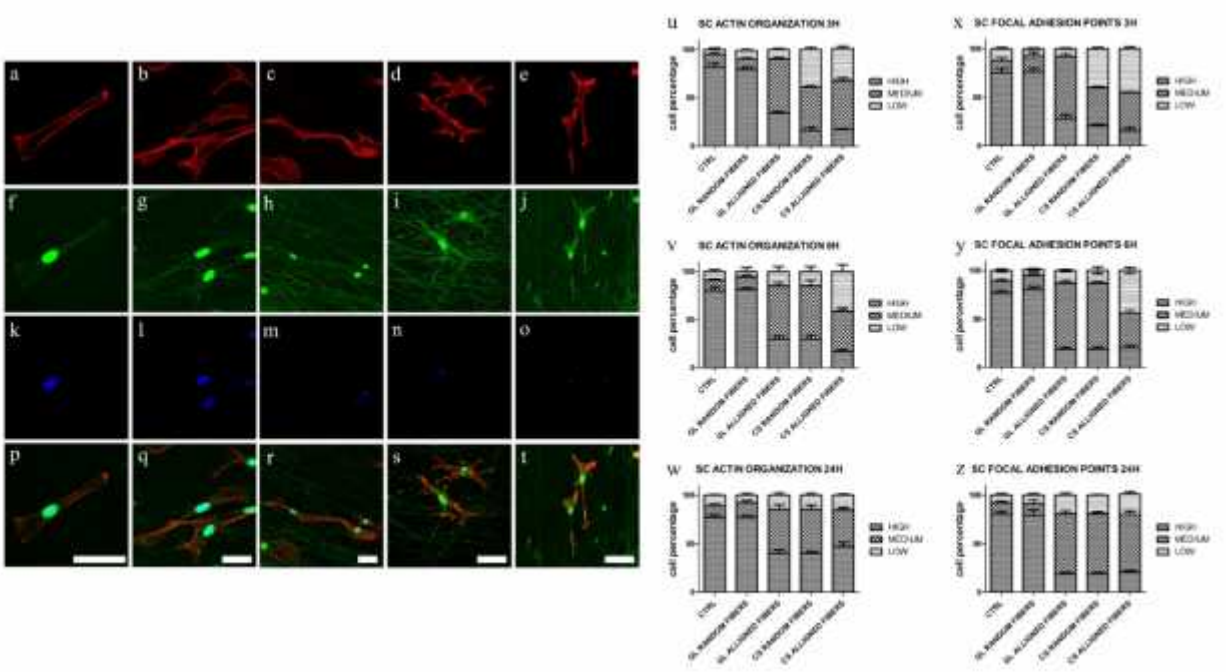

Figure 6. Primary SC actin cytoskeleton and focal adhesion points organization. Fluorescence images following phalloidin-actin (red), vinculin (green) and DAPI (blue) staining of SC on poly-l-lysine coated coverslips (control condition, a, f, k and p), gelatin random fibers (b, g, l and q), gelatin aligned fibers (c, h, m and r), chitosan random fibers (d, i, n and s), and chitosan aligned fibers (e, j, o and t). Fibers substrates appear green due to material autofluorescence. Images were acquired at 60X magnification with different zoom. Scale bar: 40 µm. Percentages of cells with low, medium or high actin cytoskeleton organization ± standard error of the mean (SEM) 3 (u), 6 (v) and 24 (w) h after seeding are reported. Percentages of cells with low, medium or high numbers of focal adhesion points ± standard error of the mean (SEM) 3 (x), 6 (y) and 24 (z) h after seeding are also reported. One-way ANOVA was used for statistical analysis. Asterisks denote statistically significant differences with *p ≤ 0.05, **p ≤ 0.01 and ***p ≤ 0.001 (Supplementary tables 17-22).

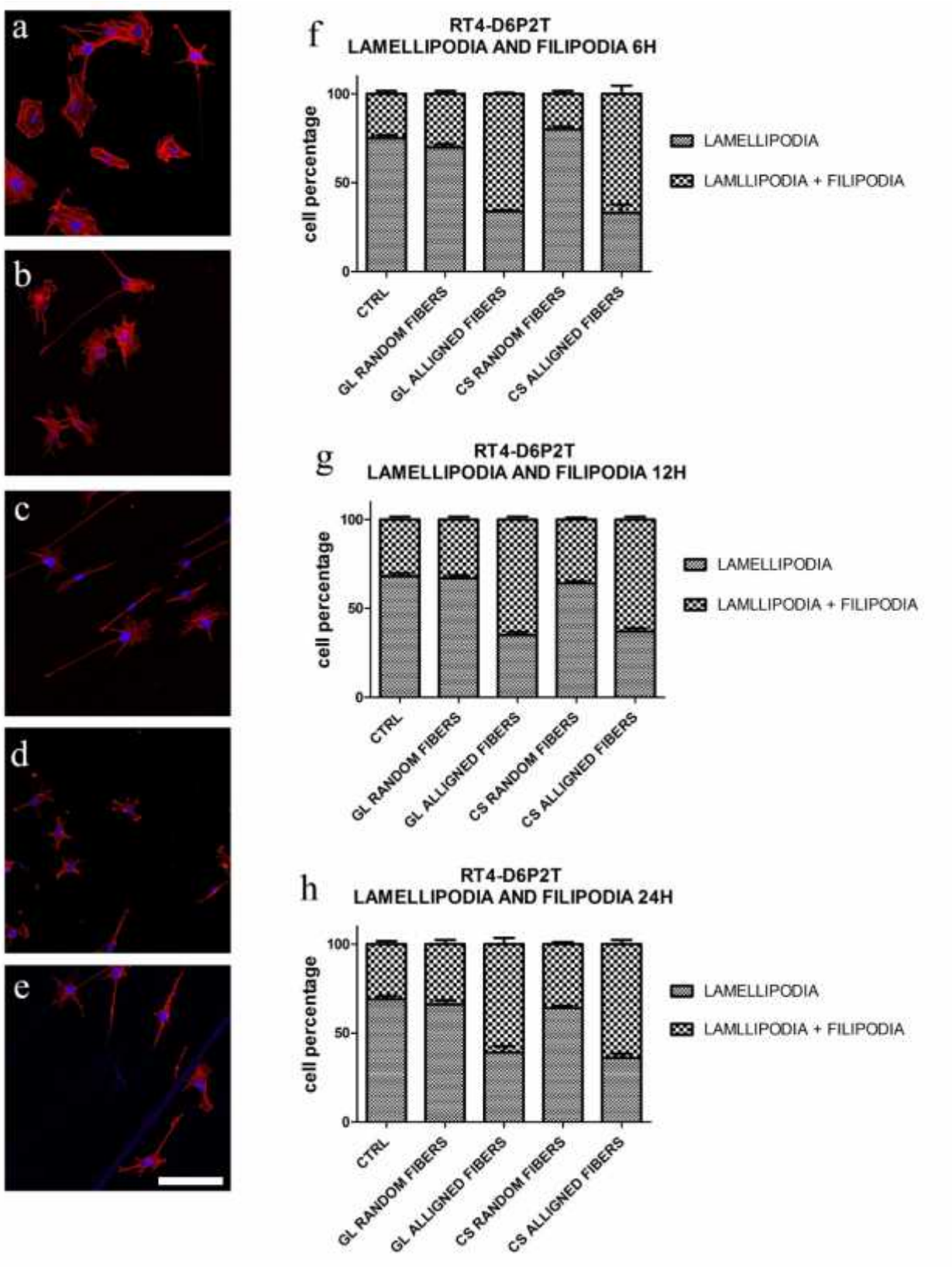

Figure 7. Lamellipodia and filopodia organization in RT4-D6P2T cells. Fluorescence images phalloidin (red) and DAPI (blue) staining of RT4-D6P2T seeded on poly-l-lysine coated coverslips (control condition, a), gelatin random fibers (b), gelatin aligned fibers (c), chitosan random fibers (d), and chitosan aligned fibers

(e) 6 hours after seeding. Images were acquired at 40X magnification. Scale bar: 100 µm. Percentage of RT4-D6P2T cells characterized by lamellipodium and filopodia protrusions 3 (f), 6 (g) and 24 (h) h after seeding are expressed as mean ± standard error of the mean (SEM). One-way ANOVA was used for statistical analysis. Asterisks denote statistically significant differences with *$p \leq 0.05$, **$p \leq 0.01$ and ***$p \leq 0.001$ (Supplementary tables 23-25).

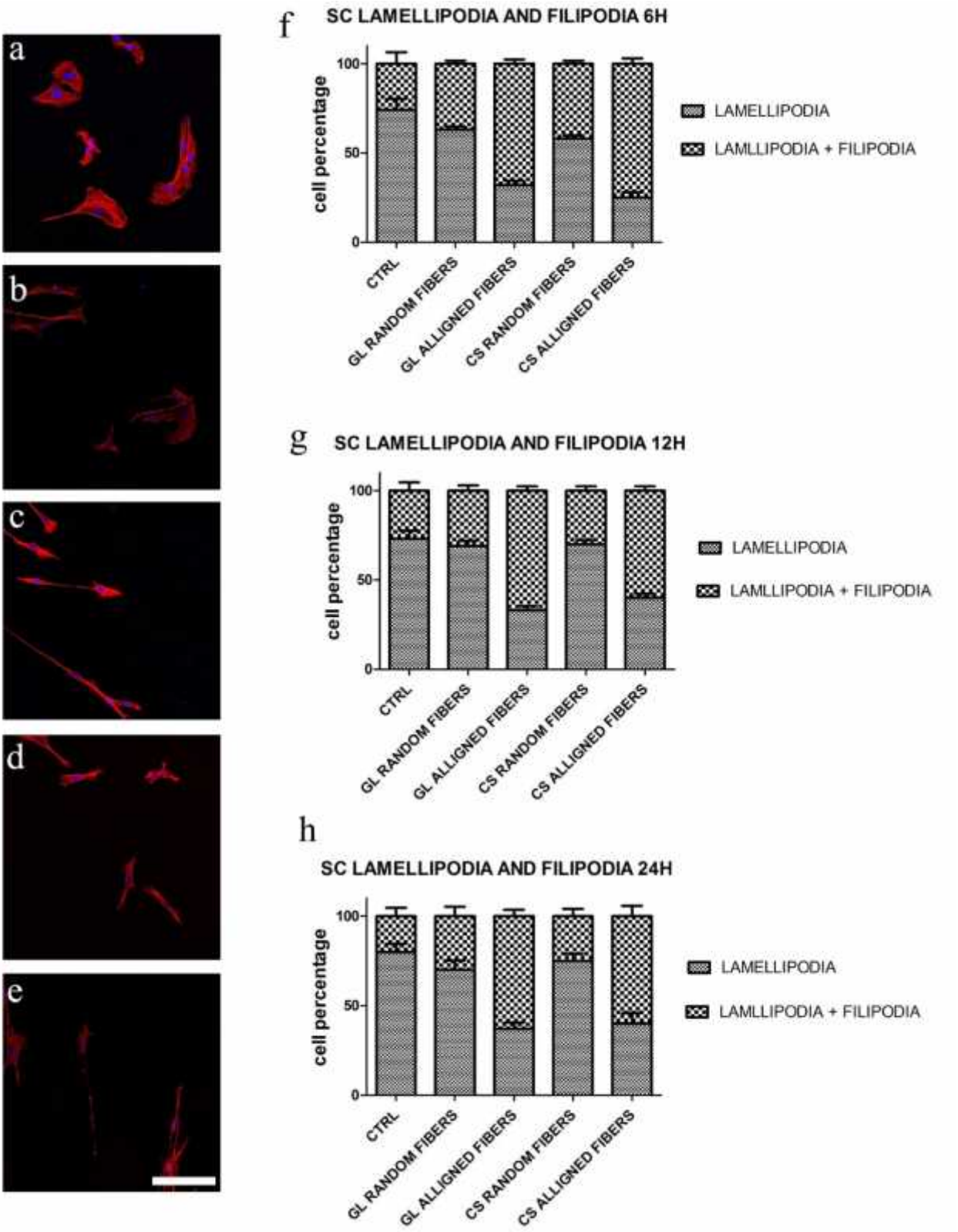

Figure 8. Lamellipodia and filopodia organization in primary SC. Fluorescence images phalloidin (red) and DAPI (blue) staining of SC seeded on poly-l-lysine coated coverslips (control condition, a), gelatin random fibers (b), gelatin aligned fibers (c), chitosan random fibers (d), and chitosan aligned fibers (e) 6 hours after

seeding. Images were acquired at 40X magnification. Scale bar: 100 µm. Percentage of SC characterized by lamellipodium and filopodia protrusions 3 (f), 6 (g) and 24 (h) h after seeding are expressed as mean ± standard error of the mean (SEM). One-way ANOVA was used for statistical analysis. Asterisks denote statistically significant differences with *$p \leq 0.05$, **$p \leq 0.01$ and ***$p \leq 0.001$ (Supplementary tables 26-28) .

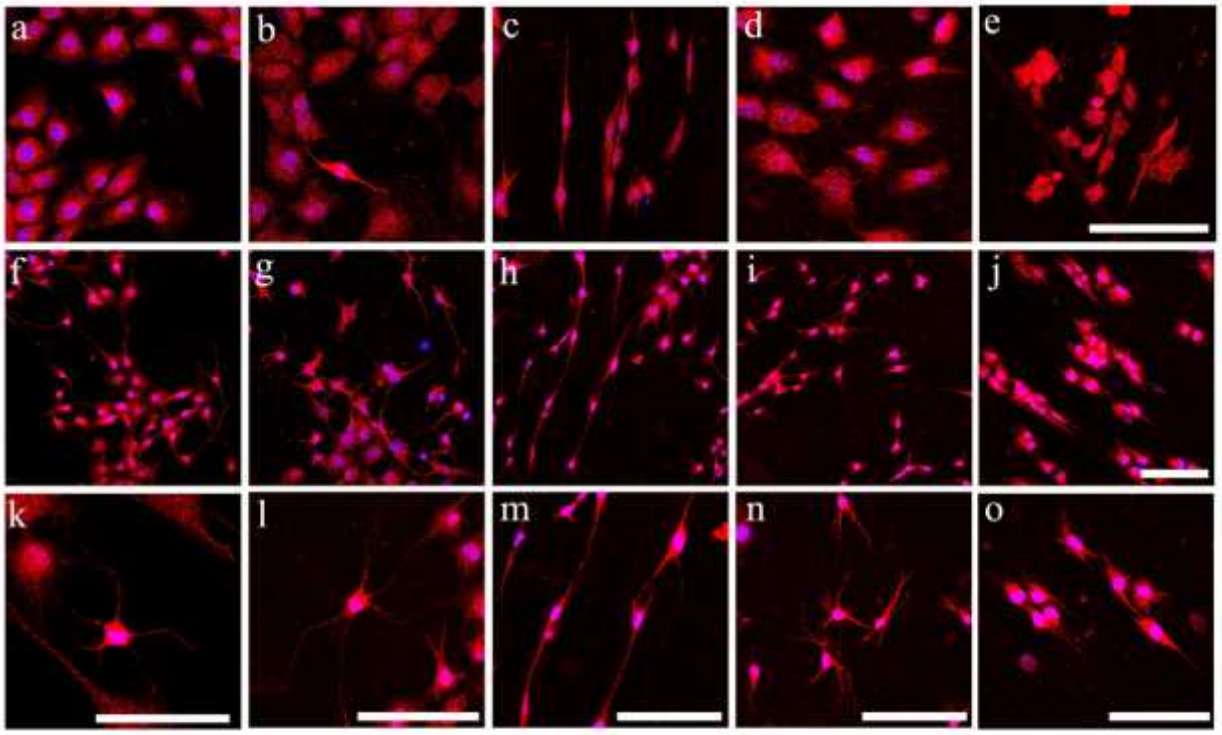
a
b
c
d
e
f
g
h
i
j
k
l
m
n
o

p

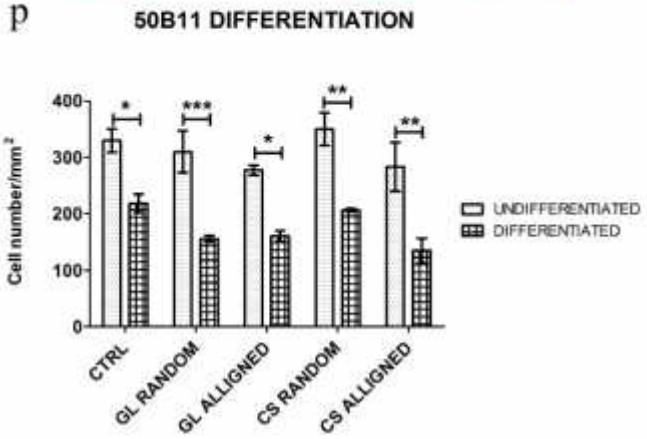
50B11 DIFFERENTIATION
Cell number/mm²
400
300
200
100
0
*
***
*
**
**
UNDIFFERENTIATED
DIFFERENTIATED
CTRL
GL RANDOM
GL ALLIGNED
CS RANDOM
CS ALLIGNED

q

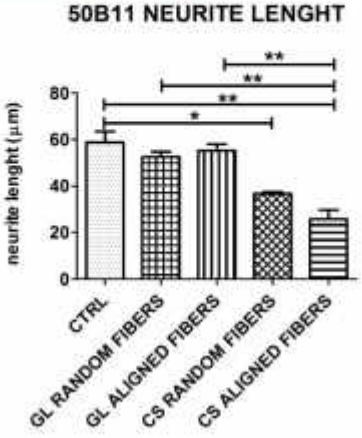
50B11 NEURITE LENGHT
neurite lenght (μm)
80
60
40
20
0
**
**
**
*
CTRL
GL RANDOM FIBERS
GL ALIGNED FIBERS
CS RANDOM FIBERS
CS ALIGNED FIBERS

r

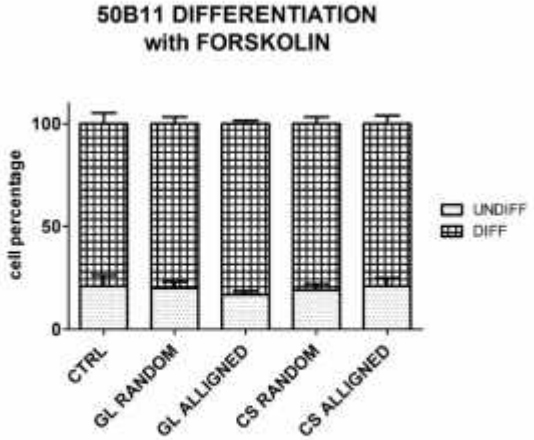
50B11 DIFFERENTIATION
with FORSKOLIN
cell percentage
100
50
0
UNDIFF
DIFF
CTRL
GL RANDOM
GL ALLIGNED
CS RANDOM
CS ALLIGNED

s

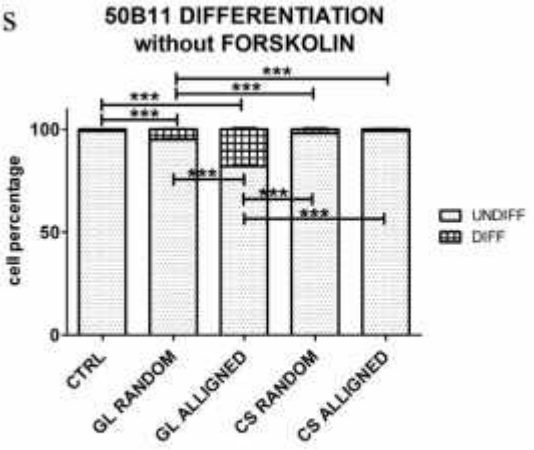
50B11 DIFFERENTIATION
without FORSKOLIN
cell percentage
100
50
0
***
***
***
***
***
***
***
UNDIFF
DIFF
CTRL
GL RANDOM
GL ALLIGNED
CS RANDOM
CS ALLIGNED

Figure 9. 50B11 differentiation: Confocal images after β-tubulin (red) and DAPI (blue) staining of B5011 seeded on poly-l-lysine coated coverslips (control condition, a, f, and k), random gelatin fibers (b, g, and l), aligned gelatin fibers (c, h and m), random chitosan fibers (d, I and n) and aligned chitosan fibers (e, j and o). 50B11 cells were cultured without (a-e) or with forskolin (f-o) addition to the culture medium Images were acquired at 40X or 60X magnification with different zoom. Scale bar: 100 µm. 50B11 cell were counted and cell number is expressed as cells/mm^2 ± standard error of the mean (SEM) (p); Neurite length is expressed in µm± standard error of the mean (SEM) (q); 50B11 differentiated and undifferentiated cells in presence (r) or without (s) forskolin treatment are expressed as percentage of cells± standard error of the mean (SEM). One way ANOVA was used for statistical analysis. Asterisks reported in figure refer to significant statistical difference with * $p \leq 0.05$, ** $p \leq 0.01$ and *** $p \leq 0.001$. Two-way ANOVA was also used for statistical analysis. Asterisks refer to significant statistical difference with * $p \leq 0.05$, ** $p \leq 0.01$ and *** $p \leq 0.001$ (Supplementary tables 8-10).

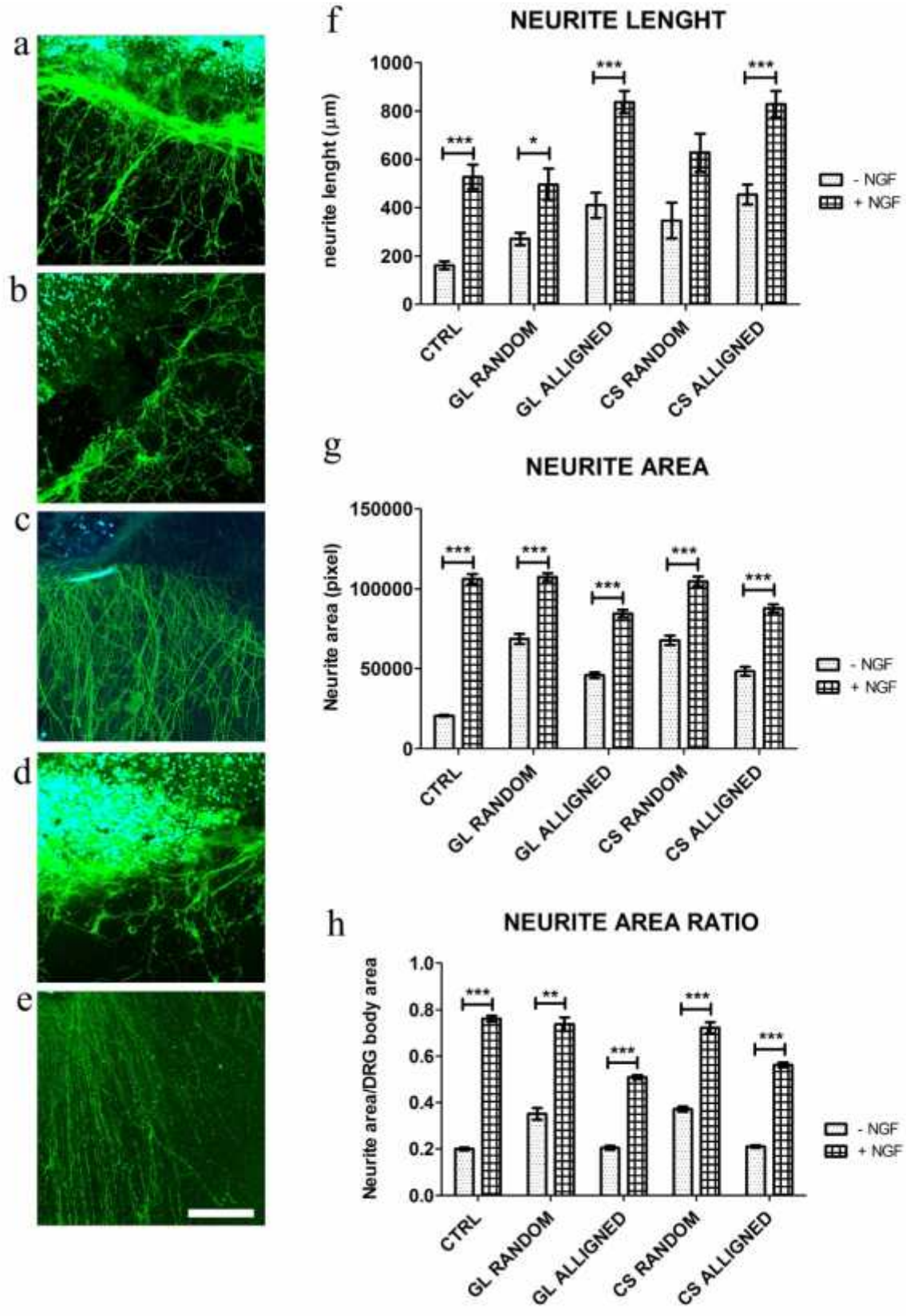

Figure 10. Fluorescence images after β-tubulin (green) and DAPI (blue) staining of DRG explants cultured on control condition (polylysine coated coverslips, a), random gelatin fibers (b), aligned gelatin fibers (c), random chitosan fibers (d) and aligned chitosan fibers (e) without (not shown) or with NGF (a-e). Images

were acquired at 40X magnification. Scale bar: 100 µm. Axon length expressed as µm ± standard error of the mean (SEM) (f), density as pixel ± SEM (g), sprouting area as DRG axon area/DRG axon area ratio ± SEM (h). One way ANOVA was used for statistical analysis. Asterisks reported in figure refer to significant statistical difference with * $p \leq 0.05$, ** $p \leq 0.01$ and *** $p \leq 0.001$. Two-way ANOVA was also used for statistical analysis. Asterisks refer to significant statistical difference with * $p \leq 0.05$, ** $p \leq 0.01$ and *** $p \leq 0.001$ (Supplementary tables 5-7).